JOURNAL OF COMPUTATIONAL PHYSICS 105, 267–278 (1993)

Laplace's Equation and the Dirichlet–Neumann Map in Multiply Connected Domains*

A. GREENBAUM AND L. GREENGARD

Courant Institute of Mathematical Sciences New York University, New York, New York 10012

AND

G. B. MCFADDEN

Computing and Applied Mathematics Laboratory, National Institute of Standards and Technology, Gaithersburg, Maryland 20899

Received July 22, 1991; revised August 10, 1992

A variety of problems in materials science and fluid dynamics require the solution of Laplace's equation in multiply connected domains. Integral equation methods are natural candidates for such problems, since they discretize the boundary alone, require no special effort for free boundaries, and achieve superalgebraic convergence rates on sufficiently smooth domains in two space dimensions, regardless of shape. Current integral equation methods for the Dirichlet problem, however, require the solution of M independent problems of dimension N, where M is the number of boundary components and N is the total number of points in the discretization. In this paper, we present a new boundary integral equation approach, valid for both interior and exterior problems, which requires the solution of a single linear system of dimension $N+M$. We solve this system by making use of an iterative method (GMRES) combined with the fast multipole method for the rapid calculation of the necessary matrix vector products. For a two-dimensional system with 200 components and 100 points on each boundary, we gain a speedup of a factor of 100 from the new analytic formulation and a factor of 50 from the fast multipole method. The resulting scheme brings large scale calculations in extremely complex domains within practical reach.

1. INTRODUCTION

Several problems in applied mathematics involve the solution of Laplace's equation in multiply connected domains. Examples arise in fluid dynamics, electrostatics, and various aspects of materials science (see, for example, [2, 6, 12, 14, 17, 19, 20, 27, 28]). In some circumstances, the solution is desired at a set of points in the interior of the domain. In other circumstances, values of the normal derivative are to be derived from a specification of function values on the boundary (the Dirichlet–Neumann map). In the numerical treatment of such problems, second kind integral equation methods are a natural choice, having a number of advantages over finite difference or finite element discretizations. The latter require a discretization of the entire computational domain, are difficult to apply to exterior problems, lead to poorly conditioned linear systems, and achieve a low order of accuracy, although the resulting matrices are sparse and amenable to efficient solution by, for example, a multigrid procedure. Second kind integral equation methods require a discretization of the boundary alone (so that the size of the resulting linear system is drastically reduced), achieve superalgebraic convergence on smooth two-dimensional domains, are as easily applied to exterior as to interior problems and are well conditioned. They do, however, give rise to dense matrices.

In simply connected domains, the most obvious method for solving the linear systems which result from discretizing integral equations is Gaussian elimination, which requires $O(N^3)$ operations, where N is the number of points on the boundary. On the other hand, a number of authors have observed that since such systems are well-conditioned, iterative methods are easily applied and achieve a fixed accuracy in a number of iterations independent of N (see, for example, [2, 7, 22]). Each iteration, of course, would appear to require $O(N^2)$ operations so that the net cost of solving the linear system would be $O(N^2)$. During the past few years, however, several schemes have appeared which reduce the cost of each iteration to $O(N \log N)$ or $O(N)$ [1, 4, 5, 10, 11, 21, 22, 26], and their application results in

* The first two authors were supported by the Applied Mathematical Sciences Program of the U.S. Department of Energy under Contract DEFGO288ER25053. The second author was also supported by a NSF Presidential Young Investigator Award and by a Packard Foundation Fellowship. The third author was supported by the NASA Microgravity Science and Applications Program and by the DARPA Applied and Computational Mathematics Program.

0021-9991/93 $5.00

optimal order methods for solving Laplace's equation. Of particular note is the paper of Rokhlin [22], in which such a hybrid method first appeared.

In multiply connected domains, unfortunately, the situation is not so simple. Second kind integral equation methods for the Dirichlet problem develop a nullspace of dimension equal to the number of boundary components M. In order to obtain a solution, therefore, one of two strategies has been employed. The first is to project the Dirichlet data onto the range of the operator by subjecting the data to certain compatibility constraints (see, for example, [3, 17]). While the algorithms of [3, 17] differ in several details, both require the solution of M adjoint integral equations, each of dimension N, where N is the number of points in the discretization of the entire boundary. An alternative approach, due to Mayo [15], uses a modified integral equation described by Mikhlin [19]. This scheme does not require solutions of the adjoint equation, but does require the solution of M (non-singular) integral equations of dimension N. With the use of the fast summation techniques mentioned above, the work required by the methods of [3, 15, 17] is of the order $O(N \cdot M)$. For small M, they are essentially optimal order.

In this paper, we are interested in a rather different regime—where M is large (up to several hundred), in which case the above schemes undergo a serious degradation in performance. We present an algorithm whose asymptotic CPU time requirements are of the order $O(N+M)$, $O(N+M^2)$, or $O(N+M^3)$, depending on the details of the implementation, rather than $O(N \cdot M)$. For a system with 200 components and 100 points on each boundary ($M = 200$, $N = 20{,}000$), we gain a speedup of a factor of 100 from the new analytic formulation. Another factor of 50 in speedup is gained from using the fast multipole method [5, 10, 22] to apply the discretized integral operators. The resulting scheme brings large scale calculations in extremely complex domains within practical reach.

One important issue we do not discuss is that of evaluating the solution at a large number of points (off the boundary) once the integral equation has been solved. Mayo [15, 16] has introduced a fast, robust method for this purpose which requires only $O(N+n^2 \log n)$ work to obtain the solution at all points of an $n \times n$ grid in which the physical domain is embedded. We plan to incorporate this method at a later date.

The paper is organized as follows: Section 2 reviews the integral equation approach to the Dirichlet problem in simply connected domains, Section 3 extends the analysis to multiply connected domains, and Section 4 describes our numerical method in some detail. Section 5 explains how to obtain the Dirichlet–Neumann map and how to solve the Neumann problem, Section 6 presents the results of some numerical experiments, and Section 7 contains our conclusions.

2. SIMPLY CONNECTED DOMAINS

We will briefly describe the solution of the Dirichlet problem for Laplace's equation in simply connected domains via classical potential theory. Descriptions of this theory may be found, for example, in [8, 9, 13, 19].

Let us begin by considering a finite open region D in the plane with boundary L, which we assume to be smooth and to have continuous curvature. We denote by E the open region in the plane exterior to L. The interior Dirichlet problem, then, involves the determination of a function $U(P)$ which satisfies

$$\Delta U(P) = 0 \qquad \text{for} \quad P \in D \tag{1}$$

and the boundary condition

$$\lim_{\substack{P \to Q \\ P \in D}} U(P) = f(Q) \qquad \text{for} \quad Q \in L. \tag{2}$$

We seek the solution $U(P)$ in the form of a double layer potential

$$U(P) = \frac{1}{2\pi} \int_L \mu(Q) \frac{\partial}{\partial \nu_Q} \ln |Q - P| \, dQ, \tag{3}$$

where P is a point inside D, $\mu(Q)$ is the value of the unknown dipole distribution at the boundary point Q, and $\partial/\partial \nu_Q$ represents the outward normal derivative at the point Q.

For any point Q_0 on the boundary, the double layer potential satisfies the jump relations

$$\lim_{\substack{P \to Q_0 \\ P \in D}} U(P) = \frac{1}{2}\mu(Q_0) + \frac{1}{2\pi} \int_L \mu(Q) \times \frac{\partial}{\partial \nu_Q} \ln |Q - Q_0| \, dQ \tag{4}$$

$$\lim_{\substack{P \to Q_0 \\ P \in E}} U(P) = -\frac{1}{2}\mu(Q_0) + \frac{1}{2\pi} \int_L \mu(Q) \times \frac{\partial}{\partial \nu_Q} \ln |Q - Q_0| \, dQ. \tag{5}$$

In order to satisfy the boundary condition (2), the relation (4) implies that the function μ must satisfy the integral equation

$$\mu(Q_0) + \frac{1}{\pi} \int_L \mu(Q) \frac{\partial}{\partial \nu_Q} \ln |Q - Q_0| \, dQ = 2f(Q_0). \tag{6}$$

We note that the kernel $(\partial/\partial\nu_Q) \ln |Q - Q_0|$ is continuous along the curve; in fact, for future reference,

$$\lim_{\substack{Q \to Q_0 \\ Q \in L}} \frac{\partial}{\partial \nu_Q} \ln |Q - Q_0| = \frac{1}{2} \kappa(Q_0), \tag{7}$$

where $\kappa(Q)$ denotes the curvature of L at the point Q. Moreover, it is well known that Eq. (6) has no nontrivial homogeneous solutions. We may, therefore, conclude from the Fredholm alternative that (6) has a unique solution for any integrable data $f(Q)$.

For the exterior Dirichlet problem,

$$\begin{aligned} &\Delta U(P) = 0 \qquad \text{for} \quad P \in E \\ &\lim_{\substack{P \to Q \\ P \in E}} U(P) = f(Q) \qquad \text{for} \quad Q \in L, \end{aligned} \tag{8}$$

U bounded, we encounter an obvious difficulty if we seek the solution in terms of a double layer potential alone. Such a representation decays to zero in the far field, while the appropriate condition at infinity is that U should tend to a constant. If we were to try to use the same double layer potential as before, the jump relation (5) would yield the integral equation

$$-\mu(Q_0) + \frac{1}{\pi} \int_L \mu(Q) \frac{\partial}{\partial \nu_Q} \ln |Q - Q_0| \, dQ = 2f(Q_0). \tag{9}$$

The Fredholm alternative still applies, of course, but the homogeneous equation now has the nontrivial solution $\mu = C$, a constant. Let us, therefore, seek a slightly different representation, namely

$$\begin{aligned} U(P) &= \frac{1}{2\pi} \int_L \mu(Q) \frac{\partial}{\partial \nu_Q} \ln |Q - P| \, dQ \\ &\quad + \frac{1}{2\pi} \int_L \mu(Q) \, dQ \\ &= \frac{1}{2\pi} \int_L \mu(Q) \left[\frac{\partial}{\partial \nu_Q} \ln |Q - P| + 1 \right] dQ. \end{aligned} \tag{10}$$

The integral equation resulting from application of the jump relation (5) is then

$$-\mu(Q_0) + \frac{1}{\pi} \int_L \mu(Q) \left[\frac{\partial}{\partial \nu_Q} \ln |Q - Q_0| + 1 \right] dQ = 2f(Q_0). \tag{11}$$

A proof of the fact that (11) has a unique solution for any integrable data $f(Q)$ can be found in [19]. We should note that logarithmic growth in the far field is also a well-posed radiation condition. This possibility is discussed briefly in Section 3.2.

3. MULTIPLY CONNECTED DOMAINS

Let us now consider the Dirichlet problem in a finite open region D in the plane which is $(M+1)$-ply connected (Fig. 1). The outer boundary of D will be denoted by L_0, while the interior boundary curves will be denoted by $L_1, \ldots, L_M$. If we seek the solution $U(P)$ as a double layer potential, and use the jump relation (4), we obtain the integral equation

$$\mu(Q_0) + \frac{1}{\pi} \int_L \mu(Q) \frac{\partial}{\partial \nu_Q} \ln |Q - Q_0| \, dQ = 2f(Q_0), \tag{12}$$

where $f(Q)$ is the given boundary data.

Remark 3.1. We will follow the standard convention that for *interior* problems, $\partial/\partial\nu_Q$ refers to the normal derivative in the direction outward from the domain D. Thus, whether the boundary point Q_0 lies on the outer boundary or on one of the interior curves, the relevant jump condition is (4). For *exterior* problems, $\partial/\partial\nu_Q$ refers to the inward normal derivative and the relevant jump condition is (5).

There is a fundamental problem with the linear system (12), which is that there are M nontrivial homogeneous solutions of the form

$$\xi_i(Q) = \begin{cases} 1 & \text{for} \quad Q \in L_i, \\ 0 & \text{for} \quad Q \in L_k, \, k \neq i, \end{cases} \qquad i = 1, \ldots, M.$$

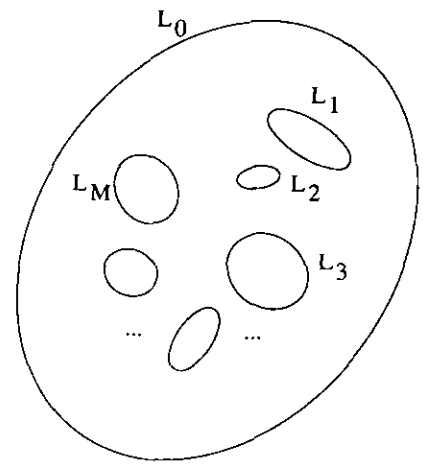

FIG. 1. A bounded multiply connected domain D in the plane. The outer boundary of D is denoted by L_0, while the interior boundary curves are denoted by $L_1, \ldots, L_M$.

That they are null solutions follows immediately from the identity

$$\frac{1}{2\pi}\int_{L_i}\frac{\partial}{\partial v_Q}\ln|Q-Q_0|\,dQ = \begin{cases} -1 & \text{for } Q_0 \text{ inside } L_i \\ -\frac{1}{2} & \text{for } Q_0 \text{ on } L_i \\ 0 & \text{for } Q_0 \text{ outside } L_i. \end{cases}$$

For a proof that they *span* the nullspace, see [8].

In short, we may conclude from Fredholm theory that Eq. (12) can be solved only if the right-hand side is *orthogonal to the M independent solutions of the adjoint* integral equation

$$\sigma(Q_0)+\frac{1}{\pi}\int_L \sigma(Q)\frac{\partial}{\partial v_{Q_0}}\ln|Q-Q_0|\,dQ=0.$$

This approach is the one taken in [3, 17] and requires the determination of the M independent solutions of the adjoint system.

3.1. *A Direct Formulation*

A somewhat different approach to the multiply-connected problem is suggested by Mikhlin [19]. Rather than making use of the general Fredholm theory, as we did above, let us seek a solution in the form

$$U(P)=\frac{1}{2\pi}\int_L \mu(Q)\frac{\partial}{\partial v_Q}\ln|Q-P|\,dQ + \sum_{k=1}^{M} A_k \ln|P-S_k|, \tag{13}$$

where S_k is a point inside the interior boundary curve L_k. In the context of fluid dynamics, the unknown constants A_k correspond to circulation, but we will think of them as playing the role of Lagrange multipliers. Applying the jump relations as before, the resulting integral equation is

$$\mu(Q_0)+\frac{1}{\pi}\int_L \mu(Q)\frac{\partial}{\partial v_Q}\ln|Q-Q_0|\,dQ = 2f(Q_0)-2\sum_{k=1}^{M} A_k \ln|Q_0-S_k|. \tag{14}$$

As an integral equation for the dipole distribution μ, the rank deficiency encountered previously is still present. We have only modified the right-hand side. The next step, however, is to replace Eq. (14) by

$$\mu(Q_0)+\frac{1}{\pi}\int_L \mu(Q)\left[\frac{\partial}{\partial v_Q}\ln|Q-Q_0|+S(Q,Q_0)\right]dQ = 2f(Q_0)-2\sum_{k=1}^{M} A_k \ln|P-S_k|, \tag{15}$$

where

$$S(Q,Q_0)=\begin{cases}1 & \text{if } Q, Q_0 \in L_k,\ k=1,\ldots,M \\ 0 & \text{otherwise.}\end{cases}$$

This modification of the kernel adds a term of the form

$$\frac{1}{\pi}\int_{L_k}\mu(Q)\,dQ$$

to Eq. (14) if and only if Q_0 lies on an interior boundary curve L_k. The value of this modification is that the integral equation (15) is nonsingular—it has a unique solution for any integrable right-hand side. A proof may be found in [19].

Notice, however, that we have made no use as yet of the unknown constants A_k. Given these M extra degrees of freedom, we may subject the system (15) to the constraint conditions

$$\int_{L_k}\mu(Q)\,dQ=0, \qquad k=1,\ldots,M. \tag{16}$$

But then (15) and (14) are identical, so that we have constructed a solution to our problem in the desired form (13).

Let us, therefore, consider a single system of equations, namely (14) and (16) taken together and rewritten in the form

$$\mu(Q_0)+\frac{1}{\pi}\int_L \mu(Q)\frac{\partial}{\partial v_Q}\ln|Q-Q_0|\,dQ + 2\sum_{k=1}^{M} A_k \ln|Q_0-S_k| = 2f(Q_0) \tag{17}$$

$$\int_{L_k}\mu(Q)\,dQ=0, \qquad k=1,\ldots,M.$$

By the preceding discussion, this system is invertible and simultaneously determines the values of the constant A_k and the desired dipole density $\mu(Q)$.

3.2. *The Exterior Problem*

Let E be the open region in the plane exterior to M closed curves $L_1, \ldots, L_M$ (Fig. 2). As suggested by Mikhlin [19], we seek a solution in the form

$$U(P)=\frac{1}{2\pi}\int_L \mu(Q)\frac{\partial}{\partial v_Q}\ln|Q-P|\,dQ+\frac{1}{2\pi}\int_L \mu(Q)\,dQ + \sum_{k=1}^{M} A_k \ln|P-S_k|, \tag{18}$$

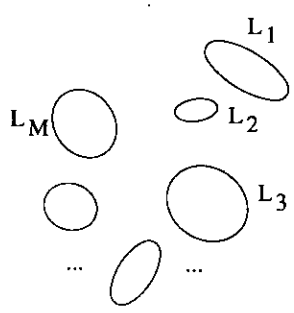

FIG. 2. An unbounded multiply connected domain E in the plane. The boundaries of the M holes are denoted by $L_1, ..., L_M$.

where S_k is a point inside the boundary curve L_k. We will require that

$$\sum_{k=1}^{M} A_k = 0 \tag{19}$$

to ensure that U is bounded at infinity. (If the desired behavior in the far field is that the solution grow like $A \log r$ rather than tend to a constant, one can simply set $\sum_{k=1}^{M} A_k = A$.)

Application of the jump relation (5) yields the integral equation

$$-\mu(Q_0) + \frac{1}{\pi}\int_L \mu(Q)\frac{\partial}{\partial \nu_Q}\ln|Q-Q_0|\,dQ + \frac{1}{\pi}\int_L \mu(Q)\,dQ = 2f(Q_0) - 2\sum_{k=1}^{M} A_k \ln|Q_0 - S_k|, \tag{20}$$

which has $M-1$ nontrivial homogeneous solutions. This equation can be modified as above, replacing Eq. (20) with

$$-\mu(Q_0) + \frac{1}{\pi}\int_L \mu(Q) \times\left[\frac{\partial}{\partial \nu_Q}\ln|Q-Q_0| + R(Q, Q_0)\right] dQ + \frac{1}{\pi}\int_L \mu(Q)\,dQ = 2f(Q_0) - 2\sum_{k=1}^{M} A_k \ln|Q_0 - S_k|, \tag{21}$$

where

$$R(Q, Q_0) = \begin{cases} 1 & \text{if } Q, Q_0 \in L_k,\ k = 1, ..., M-1 \\ 0 & \text{otherwise.} \end{cases}$$

Note that the Mth boundary curve is distinguished from the others in the definition of $R(Q, Q_0)$. The value of this modification of the kernel is that, as for the interior problem, the resulting system (21) is invertible (see [19]).

We now make use of the unknown constants A_k. Since we have already required that they satisfy (19), we are left with $M-1$ degrees of freedom. We may, therefore, subject the preceding linear system to the constraints

$$\int_{L_k} \mu(Q)\,dQ = 0, \qquad k = 1, ..., M-1. \tag{22}$$

Equations (20) and (21) are then identical, and we have constructed a solution to the exterior problem in the form (18). Rewriting (19), (20), and (22) as a simultaneous set of equations for the unknown constants A_k and the unknown dipole density μ, we have

$$\mu(Q_0) - \frac{1}{\pi}\int_L \mu(Q)\left[\frac{\partial}{\partial \nu_Q}\ln|Q-Q_0| + 1\right] dQ - 2\sum_{k=1}^{M} A_k \ln|Q_0 - S_k| = -2f(Q_0)$$

$$\sum_{k=1}^{M} A_k = 0 \tag{23}$$

$$\int_{L_k} \mu(Q)\,dQ = 0, \qquad k = 1, ..., M-1.$$

4. FORMULATION OF NUMERICAL METHOD

In order to solve the systems (17) and (23), we use the Nyström algorithm based on the trapezoidal rule. We use the trapezoidal rule for quadrature since it achieves super-algebraic convergence for smooth funcions on periodic domains. In more detail, we assume that we are given N_k points equispaced in arclength on each boundary component L_k and associate with each such point, denoted Q_i^k, an unknown density value μ_i^k. The step in arclength in the discretization of L_k will be denoted $h_k = |L_k|/N_k$, where $|L_k|$ is the length of the curve L_k. The total number of discretization points is denoted by

$$N = \sum_{k=1}^{M} N_k \qquad \text{for the exterior problem}$$

$$N = \sum_{k=0}^{M} N_k \qquad \text{for the interior problem.}$$

We then replace Eq. (17) by

$$\mu_i^l + \frac{1}{\pi}\sum_{k=0}^{M} h_k \sum_{j=1}^{N_k} \frac{\partial}{\partial \nu_{Q_j^k}}\ln|Q_j^k - Q_i^l|\,\mu_j^k + 2\sum_{k=1}^{M} A_k \ln|Q_i^l - S_k| = 2f(Q_i^l) \tag{24}$$

$$\sum_{j=1}^{N_k} \mu_j^k h_k = 0, \qquad k = 1, ..., M,$$

and Eqs. (23) by

$$\begin{aligned}
&\mu_i^l - \frac{1}{\pi}\sum_{k=1}^{M} h_k \sum_{j=1}^{N_k}\left[\frac{\partial}{\partial v_{Q_j^k}}\ln|Q_j^k - Q_i^l| + 1\right]\mu_j^k \\
&\quad - 2\sum_{k=1}^{M} A_k \ln|Q_i^l - S_k| = -2f(Q_i^l) \\
&\sum_{k=1}^{M} A_k = 0 \\
&\sum_{j=1}^{N_k} \mu_j^k h_k = 0, \qquad k = 1, \ldots, M-1,
\end{aligned} \tag{25}$$

Remark 4.1. In the preceding linear systems, the diagonal terms of the form $(\partial/\partial v_{Q_j^k}) \ln|Q_j^k - Q_i^l|$ should be replaced by the appropriate limit $\kappa(Q_i^l)/2$ when $Q_j^k = Q_i^l$ in accordance with Eq. (7).

The discrete equations for the interior and exterior problems may be written respectively as

$$\begin{pmatrix} I + K^i & B^i \\ C^i & D^i \end{pmatrix}\begin{pmatrix} \mathbf{u} \\ \mathbf{a} \end{pmatrix} = \begin{pmatrix} 2\mathbf{f} \\ 0 \end{pmatrix}, \tag{26}$$

$$\begin{pmatrix} I - K^e & B^e \\ C^e & D^e \end{pmatrix}\begin{pmatrix} \mathbf{u} \\ \mathbf{a} \end{pmatrix} = \begin{pmatrix} -2\mathbf{f} \\ 0 \end{pmatrix}, \tag{27}$$

where, for the interior problem,

$$\mathbf{u} = (\mu_1^0, \ldots, \mu_{N_0}^0, \mu_1^1, \ldots, \mu_{N_1}^1, \ldots, \mu_1^M, \ldots, \mu_{N_M}^M)^{\mathrm{T}}$$

is the vector of unknown density values,

$$\mathbf{a} = (A_1, \ldots, A_M)^{\mathrm{T}}$$

is the vector of unknown coefficients, and

$$\mathbf{f} = (f_1^0, \ldots, f_{N_0}^0, f_1^1, \ldots, f_{N_1}^1, \ldots, f_1^M, \ldots, f_{N_M}^M)^{\mathrm{T}}$$

is the vector of given boundary values. For the exterior problem,

$$\boldsymbol{\mu} = (\mu_1^1, \ldots, \mu_{N_1}^1, \ldots, \mu_1^M, \ldots, \mu_{N_M}^M)^{\mathrm{T}}$$

and

$$\mathbf{f} = (f_1^1, \ldots, f_{N_1}^1, \ldots, f_1^M, \ldots, f_{N_M}^M)^{\mathrm{T}}.$$

The N by N matrices K^i and K^e in (26) and (27) represent the interactions of the discrete double layer potentials. The N by M matrices B^i and B^e represent the logarithmic terms coupling the density values to the coefficients $A_1, \ldots, A_M$. Finally, the M by N matrices C^i and C^e and the M by M matrices D^i and D^e represent the discrete constraint equations (24) and (25).

Remark 4.2. In some circumstances, it may be desirable to adopt a nonuniform mesh spacing to accomodate regions of high local curvature, near impingement of neighboring boundaries, etc. This is easily accomplished by employing suitable stretchings of the arclength coordinate.

4.1. *Solution of the Discrete Systems*

The matrix equations (26) and (27) were solved iteratively, using the generalized minimum residual method GMRES [23]. The convergence rate of this scheme depends on the eigenvalues of the matrix. More specifically, real and clustered eigenvalues are advantageous, enabling convergence in a small number of iterations.

Observation 4.1. Since the integral operators in (17) and (23) are compact, they can be approximated to any finite precision by an operator of finite rank. As a result, the eigenvalues of the matrices $I + K^i$ and $I - K^e$ can be shown to be asymptotically bounded and to cluster around one. In the continuous case they are real, despite the fact that the matrices are nonsymmetric (see [13]).

DEFINITION 4.1. Because of the preceding observation, we will say that $I + K^i$ and $I - K^e$ are *effectively low rank* perturbations of the identity.

The full matrices in (26) and (27) can also be viewed as effectively low rank perturbations of the identity. The rank of the perturbation may grow, however, as the blocks B, C, and D grow in dimension (with increasing numbers of components) and as the geometry becomes more complicated (affecting the spectral behavior of K^i and K^e).

In order to obtain a matrix whose eigenvalues are better distributed for iterative methods such as GMRES, a preconditioner can be used. Thus, instead of solving the linear systems in (26) and (27), we solve the systems

$$\begin{aligned}
&\begin{pmatrix} I & B^i \\ C^i & D^i \end{pmatrix}^{-1}\begin{pmatrix} I + K^i & B^i \\ C^i & D^i \end{pmatrix}\begin{pmatrix} \mathbf{u} \\ \mathbf{a} \end{pmatrix} \\
&\quad = \begin{pmatrix} I & B^i \\ C^i & D^i \end{pmatrix}^{-1}\begin{pmatrix} 2\mathbf{f} \\ 0 \end{pmatrix},
\end{aligned} \tag{28}$$

and

$$\begin{aligned}
&\begin{pmatrix} I & B^e \\ C^e & D^e \end{pmatrix}^{-1}\begin{pmatrix} I - K^e & B^e \\ C^e & D^e \end{pmatrix}\begin{pmatrix} \mathbf{u} \\ \mathbf{a} \end{pmatrix} \\
&\quad = \begin{pmatrix} I & B^e \\ C^e & D^e \end{pmatrix}^{-1}\begin{pmatrix} -2\mathbf{f} \\ 0 \end{pmatrix},
\end{aligned} \tag{29}$$

It is easy to verify that these preconditioned matrices are effectively low rank perturbations of the identity, where the rank of the perturbation is determined by the integral

operator terms K^i and K^e but is no longer affected by the block matrices B^i, B^e, C^i, C^e, D^i, D^e.

Remark 4.3. In the remainder of this section, we will ignore the distinction between the interior and exterior problems and omit the superscripts i and e from B, C, D, and K.

At each iteration now, it is necessary to solve a linear system with the preconditioning matrix, so it is important that such a system be much easier to solve than the original full matrix equation. This is accomplished as follows. First we form the M by M Schur complement S of D in the preconditioner

$$\begin{pmatrix} I & B \\ C & D \end{pmatrix},$$

given by

$$S = D - CB. \tag{30}$$

We then factor S using Gaussian elimination. To solve the linear system

$$\begin{pmatrix} I & B \\ C & D \end{pmatrix}\begin{pmatrix} \mathbf{z}_\mu \\ \mathbf{z}_a \end{pmatrix} = \begin{pmatrix} \mathbf{r}_\mu \\ \mathbf{r}_a \end{pmatrix}, \tag{31}$$

we then backsolve with the triangular factors to obtain $\mathbf{z}_a$ from

$$S\mathbf{z}_a = \mathbf{r}_a - C\mathbf{r}_\mu \tag{32}$$

and use the computed value of $\mathbf{z}_a$ to obtain $\mathbf{z}_\mu$ from

$$\mathbf{z}_\mu = \mathbf{r}_\mu - B\mathbf{z}_a. \tag{33}$$

The initial factorization requires $\frac{1}{3}M^3$ operations, while backsolving requires M^2 operations at each GMRES iteration.

The bulk of the work at each iteration, however, lies in applying the full matrix to a vector. The product

$$\begin{pmatrix} I \pm K & B \\ C & D \end{pmatrix}\begin{pmatrix} \boldsymbol{\mu} \\ \mathbf{a} \end{pmatrix}$$

can be computed in time $O(N+M)$ using the adaptive fast multipole method [5], a recently developed technique for the evaluation of potential fields. In brief, the dense matrix vector product $K\boldsymbol{\mu}$ corresponds to evaluating the pairwise interactions of a collection of dipoles located at the points Q_j^k, while the dense matrix vector product $B\mathbf{a}$ corresponds to evaluating the field at the points Q_j^k due to a collection of M charges located at the points S_k. It should be mentioned that we neither form nor store the matrix K, so that the total storage requirements of the algorithm are $O(N+M^2)$, the latter term required for the preconditioning step.

5. THE DIRICHLET–NEUMANN MAP AND THE NEUMANN PROBLEM

Our approach to the Dirichlet problem leaves us with a representation of the solution $U(P)$ in the form of a double layer potential combined with a number of logarithmic sources (Eqs. (13) and (18)). The contribution to $\partial U/\partial \nu$ from the logarithmic sources can clearly be computed explicitly, while $\partial/\partial \nu$ applied to the double layer potential results in a hypersingular integral. In two dimensions, the theory of holomorphic functions can be used to simplify this calculation. We begin by observing that

$$\tilde{U}(P) = \frac{1}{2\pi}\int_L \mu(Q)\frac{\partial}{\partial \nu_Q}\ln|Q-P|\,dQ$$

is the real part of the Cauchy integral

$$\frac{1}{2\pi i}\int_L \frac{\mu(\zeta)}{\zeta - z}\,d\zeta = \tilde{U}(z) + i\tilde{V}(z),$$

where we have equated the points P and Q in the plane with the corresponding complex numbers z and ζ. $\tilde{U}$ and its harmonic conjugate $\tilde{V}$ satisfy the Cauchy–Riemann equations, so that

$$\frac{\partial \tilde{U}}{\partial \nu} = \frac{\partial \tilde{V}}{\partial \tau}$$

and it remains only to compute $\tilde{V}$ and its tangential derivative. For this purpose, we consider the boundary mesh to be divided into odd and even points. The value of $\tilde{V}$ at the odd points is then obtained by using the trapezoidal rule applied to the even points, and vice-versa. It can be shown [25] that such a rule is superalgebraically converging on smooth domains. It has been used previously by a number of authors (see, for example, [17, 18, 24]). Once $\tilde{V}$ has been tabulated, we obtain its tangential derivative via Fourier approximation in arclength and the FFT.

5.1. *The Neumann Problem*

Many important problems governed by Laplace's equation require the solution of the Neumann problem rather than the Dirichlet problem. The potential theory approach is easily applied in this case to both simply connected and multiply connected domains. We will limit our attention, for the sake of brevity, to the exterior problem; in this case, there is no large finite-dimensional nullspace which requires

special consideration. The solution of the Neumann problem

$$\begin{aligned} &\Delta U(P) = 0 \qquad \text{for} \quad P \in E, \\ &\lim_{\substack{P \to Q \\ P \in E}} \frac{\partial U(P)}{\partial \nu} = f(Q) \qquad \text{for} \quad Q \in L, \\ &\int_L f(Q)\, dQ = 0 \end{aligned} \tag{34}$$

is sought in terms of a single layer potential

$$U(P) = \frac{1}{2\pi} \int_L \sigma(Q) \ln |Q - P|\, dQ. \tag{35}$$

In order to satisfy the boundary condition at Q_0, the source density $\sigma(Q)$ must satisfy the integral equation

$$\sigma(Q_0) + \frac{1}{2\pi} \int_L \sigma(Q) \frac{\partial}{\partial \nu_{Q_0}} \ln |Q - Q_0|\, dQ = 2f(Q_0). \tag{36}$$

This equation is invertible for any permissible data $f(Q)$ (see [8]).

In the next section, we give one example of the solution of a Neumann problem, corresponding to potential flow.

6. NUMERICAL RESULTS

We illustrate the performance of the algorithm by considering both interior and exterior problems on a variety of domains.

EXAMPLE 1. $M = 6$. The Dirichlet problem is solved in a domain containing six elliptical holes (Fig. 1). The precise centers, eccentricities, and inclination angles of the ellipses are given in Table I and the data is obtained by choosing an exact solution of the form

$$U(x, y) = C + D_0 \left(\frac{x - x_0}{(x - x_0)^2 + (y - y_0)^2} \right) + \sum_{k=1}^{6} D_k \ln((x - x_k)^2 + (y - y_k)^2), \tag{37}$$

where (x_0, y_0) lies outside the outer boundary and the points (x_i, y_i), $i = 1, ..., 6$ lie inside the six holes. The latter points are distinct from the points S_k used in our method. For this example we choose

$$C = 1.0, \qquad D_k = k - \tfrac{7}{2}, \qquad k = 1, ..., 6,$$

$D_0 = 2.0$ for the interior problem, and $D_0 = 0.0$ for the exterior problem.

Figures 3a and b show the convergence of the GMRES

TABLE I

Domain in Example 1

$x(\phi) = c_x + a \cos\theta \cos\phi - b \sin\theta \sin\phi, \quad 0 \le \phi \le 2\pi$
$y(\phi) = c_y + b \cos\theta \sin\phi + a \sin\theta \cos\phi, \quad 0 \le \phi \le 2\pi$

a	b	c_x	c_y	θ
0.3626	0.1881	0.1621	0.5940	3.3108
0.5061	0.6053	−1.7059	0.3423	0.5778
0.6051	0.7078	0.3577	−0.9846	4.1087
0.7928	0.3182	1.0000	1.2668	2.6138
0.3923	0.4491	−1.9306	−1.0663	4.4057
0.2976	0.6132	−0.8330	−2.1650	5.7197
4.0000	3.0000	−0.5000	−0.5000	1.0000

Note. The first six rows correspond to the holes, while the last row corresponds to the outer boundary for the interior problem.

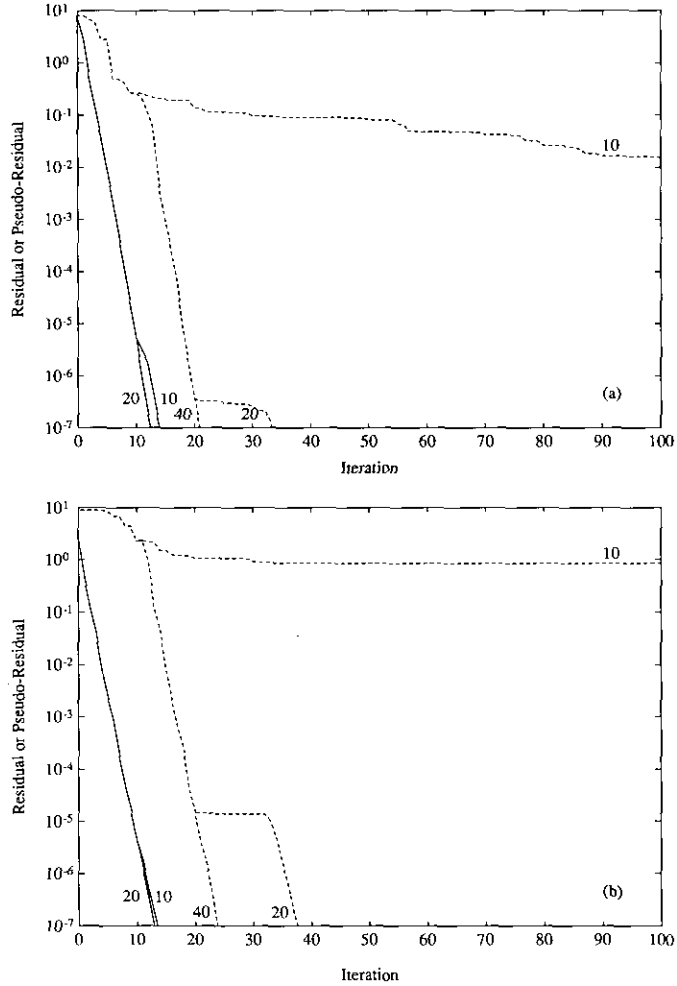

FIG. 3. The convergence rate of GMRES with and without preconditioning. (a) refers to the interior problem and (b) to the exterior problem. For the preconditioned system, the Euclidean norm of the *pseudoresidual* is plotted (the residual of the preconditioned matrix). Solid lines refer to the preconditioned system, while dashed lines refer to the unpreconditioned system. The numbers labeling the curves refer to the number of direction vectors saved before restarting.

iterative method, with and without preconditioning, for the interior and exterior problem, respectively. In each case, the right-hand side of the equations was used as the initial guess. The Euclidean norm of the residual in the preconditioned system, the *pseudoresidual* is plotted, in cases where the preconditioner was used. One hundred discretization points were used to represent each of the six interior boundaries as well as the outer boundary of the interior problem. There is one free parameter in this method, namely the number of direction vectors to be saved and orthogonalized against, before restarting the iteration. In general, saving more vectors will result in fewer iterations, but the amount of work per iteration and the amount of storage will be increased. For these problems, since the matrix vector multiply is rather expensive (typically about $100(N+M)$ operations using the fast multipole method), it makes sense, in terms of total work, to save a number of vectors. The numbers beside each curve in Fig. 3 are the number of direction vectors saved. As can be seen from the figure, if enough vectors are saved, then GMRES converges satisfactorily *with* or *without* the preconditioner. If fewer direction vectors are saved, however, the performance of the unpreconditioned algorithm is quite poor. This is approximately the behavior one would expect from the considerations outlined immediately after Observation 4.1.

The eigenvalues of the preconditioned and unpreconditioned matrices for the interior and exterior problems are plotted in Fig. 4. Note that in each case, most of the eigenvalues are tightly clustered around 1. Note also, however, that the imaginary parts of the eigenvalues of the preconditioned systems are much smaller than those of the unpreconditioned systems. This phenomenon has been observed in a wide variety of test problems, and we believe that, in the limit, as the discretization becomes finer, the eigenvalues of the preconditioned system lie on the real axis. This tends to be an advantage for the GMRES method.

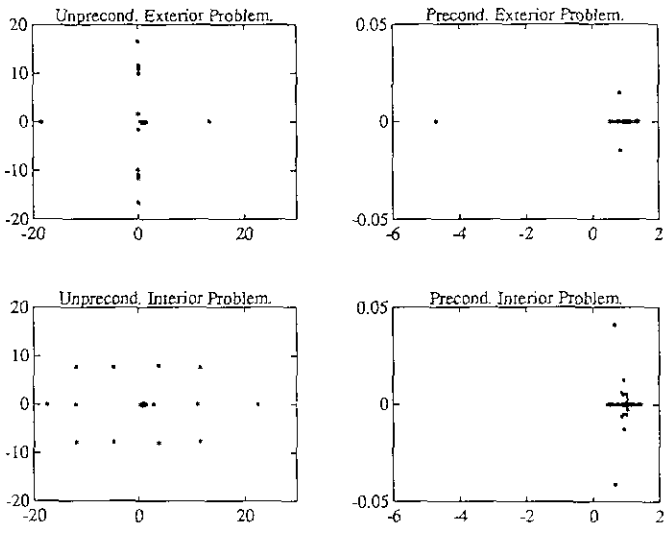

FIG. 4. Eigenvalues of the preconditioned and unpreconditioned matrices for the interior and exterior problems. Note that the eigenvalues are tightly clustered about 1, more so in the preconditioned cases. For the exterior problem, 306 eigenvalues are plotted. For the interior problem, 356 eigenvalues are plotted.

TABLE II

Performance of the Algorithm in Solving the Exterior and Interior Dirichlet Problem in Example 1

	Exterior problem			Interior problem		
N	# Iterations	CPU Time	Error	# Iterations	CPU Time	Error
50	13	23.6	0.22E−2	13	30.1	0.23E−2
100	13	67.1	0.39E−3	13	58.9	0.40E−3
200	13	130.1	0.76E−7	13	108.0	0.10E−6

Table II summarizes the performance of the algorithm as we refine the spatial discretization. The first column gives the number of points used in the discretization of each boundary. The table lists the number of preconditioned GMRES iterations (saving 20 direction vectors) required to reduce the Euclidean norm of the pseudoresidual below 10^{-7}, the CPU times in seconds required on a Sun Sparcstation 1[1] and the least squares error in computing the Dirichlet–Neumann map at all boundary discretization points. The solution was also computed at several test points inside the domain, and the error was found to be less than 10^{-7} (the accuracy to which the linear equation is solved) in each case.

The following observations can be made from Table II:

1. The number of GMRES iterations is independent of the number of discretization points used.

2. The CPU time grows linearly with the number of discretization points.

3. Convergence of the solution of the discretized problem to that of the continuous problem is superalgebraic. With 200 points per body, the discretization is accurate to at least seven decimal places.

EXAMPLE 2. $M = 200$. We next consider the region exterior to 200 randomly distributed holes in the plane, pictured in Fig. 5. (The frame around the figure is not part of the domain of the problem, but is used to identify subregions.) Each hole is a circle, with radii varying from 3.45×10^{-3} to 6.88×10^{-2}.

This type of region is typical in certain materials studies, such as the simulation of particle coarsening during Ostwald ripening [17]. In this case, particles of one material are embedded in a surrounding second-phase

[1] Reference to commercial products in this paper does not constitute recommendation or endorsment by the National Institute of Standards and Technology.

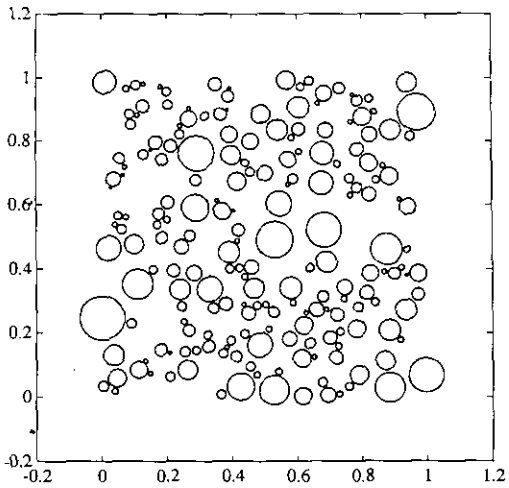

FIG. 5. A complicated exterior region, typical of certain calculations in material science, such as Ostwald ripening. There are 200 randomly distributed holes in the domain.

medium, and the problem is to follow the evolution of the interface boundary. The motion of this interface is determined by computing the Dirichlet–Neumann map with boundary condition equal to curvature. More precisely, each point on the boundary is assumed to move in the normal direction with speed given by the Neumann data.

Figures 6a and b show closeups of different sections of the domain in Fig. 5. The normal vectors on the boundaries are plotted, and their lengths represent the relative speeds at which the different boundary points move. For clarity, the velocity vectors are plotted only at every fourth boundary point. Note the tendency for the small bodies in such a configuration to shrink very rapidly, while the larger bodies grow and become non-circular.

Our discretization used 100 points per body, resulting in a matrix of order 20,200. This was solved with 11 GMRES iterations and required about 54 min on a Sun Sparcstation. Had the GMRES method been used with a conventional matrix-vector multiply routine, rather than the fast multipole method, the time required would have been about 50 h.

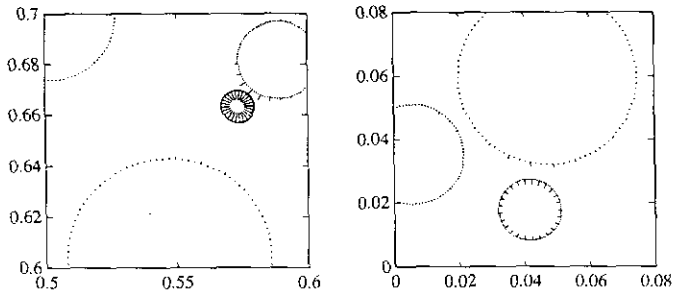

FIG. 6. Closeups of different sections of the domain of Fig. 5. Plotted are the normal vectors on the boundaries, with lengths proportional to the Neumann data generated by the Dirichlet–Neumann map. Note the tendency for small bodies to shrink rapidly and for the larger ones to grow.

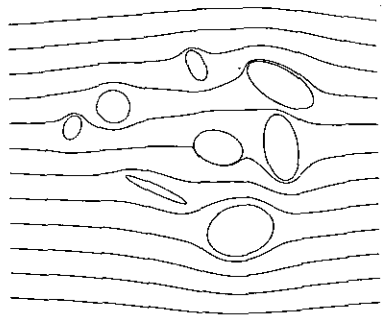

FIG. 7. Potential flow without circulation in an 8-ply connected domain.

If one used Gaussian elimination to solve this dense 20,200 by 20,200 linear system (assuming enogh storage were available to hold this matrix!), the time required would be about 3.6 months. Without the new integral equation formulation, 200 systems of dimension 20,000 would have to be solved, and even the GMRES/fast multipole iteration scheme would require more than 100 h.

EXAMPLE 3. $M = 8$. We computed potential flow in an exterior domain with eight boundary components (Fig. 7). The flow was chosen to be uniformly to the right with velocity U_0 at ∞ and to have zero circulation about each body. This allows us to represent the velocity potential as

$$\Phi(x, y) = U_0 x + \Phi_2(x, y),$$

where $\Phi_2(x, y)$ satisfies Laplace's equation with Neumann boundary conditions equal to $-\mathbf{n} \cdot (U_0, 0)$. The streamlines were computed using a fourth-order Runge–Kutta method. We should mention that in order to compute all streamlines without the use of special quadrature formulas for the evaluation of singular integrals, we overresolved the boundary, placing 2000 points on each component, resulting in a system of dimension 16,008. Sixteen iterations and 28 min were required to solve the integral equation to seven digits of accuracy.

EXAMPLE 4. $M = 6$. In this numerical experiment, we used our algorithm to compute the capacitance matrix for a system of cylindrical conductors corresponding to the exterior problem of Example 1. The entries of the capacitance matrix C are defined by

$$C_{ij} = -\frac{1}{2\pi} \int_{L_i} \frac{\partial}{\partial \nu} U^{(j)}\, ds,$$

where $U^{(j)}$ is the solution of the Dirichlet problem with boundary conditions

$$U^{(j)}(P) = 1 \quad \text{for} \quad P \in L_j$$
$$U^{(j)}(P) = 0 \quad \text{for} \quad P \in L_i,\ i \neq j.$$

Gauss' theorem shows that the constants C_{ij} are simply equal to the constants A_i (the strengths of the logarithmic sources) produced by the algorithm when used to solve Laplace's equation with the electrostatic potential fixed as above. Thus, we produce one column of the capacitance matrix with the solution of each Dirichlet problem.

Using 200 points per boundary, the capacitance matrix is given by

$$C = \begin{pmatrix} +0.835 & -0.157 & -0.467 & -0.189 & -0.012 & -0.010 \\ -0.157 & +0.701 & -0.081 & -0.104 & -0.307 & -0.053 \\ -0.467 & -0.081 & +1.070 & -0.204 & -0.054 & -0.263 \\ -0.189 & -0.104 & -0.204 & +0.556 & -0.025 & -0.035 \\ -0.012 & -0.307 & -0.054 & -0.025 & +0.717 & -0.319 \\ -0.010 & -0.053 & -0.263 & -0.035 & -0.319 & +0.680 \end{pmatrix}.$$

Each Dirichlet problem was solved to seven digits of accuracy, and the entire calculation required less than 15 min on a Sparcstation 1.

7. CONCLUSIONS

We have presented a new integral equation method for the solution of the Dirichlet problem in multiply connected domains. This new formulation has been combined with the fast multipole method to produce an algorithm capable of solving Laplace's equation in domains with hundreds of distinct boundary components in a matter of minutes on a Sparcstation 1. The asymptotic CPU time requirements of our scheme are of the order $O(N+M)$ in the unpreconditioned mode and of the order $O(N+M^3)$ in the preconditioned mode, where N is the total number of points in the boundary discretization and M is the number of distinct boundary components. When $M=200$ and $N=20{,}000$, about half the time is spent in solving the Schur complement system in the preconditioning step. As M grows further, the preconditioner, as implemented, will dominate the cost of the solution process. To be able to handle thousands of boundary components, an iterative method could be used to solve the Schur complement system rather than Gaussian elimination, but such a modification has not been implemented. We have included in our codes the ability to solve the Dirichlet problem, to compute the Dirichlet–Neumann map, and to solve the Neumann problem. We have also shown how our algorithm can be used for capacitance calculations. The method is currently being used for the simulation of Ostwald ripening, a process described briefly in Example 2 above.

While our analysis and implementation are for the two-dimensional case, there is a straightforward extension of our ideas to three dimensions, which we will report at a later date.

ACKNOWLEDGMENTS

We thank B. Braams, A. Mayo, and V. Rokhlin for several useful discussions. We also thank V. Rokhlin for providing a subroutine which allowed us to obtain a smooth resampling in arclength from a user-specified curve.

REFERENCES

1. C. R. Anderson, A method of local corrections for computing the velocity field due to a distribution of vortex blobs, *J. Comput. Phys.* **62**, 111 (1986).
2. G. R. Baker, D. I. Meiron, and S. A. Orszag, Generalized vortex methods for free-surface flow problems, *J. Fluid Mech.* **123**, 477 (1982).
3. G. R. Baker and M. J. Shelley, Boundary integral techniques for multiconnected domains, *J. Comput. Phys.* **64**, 112 (1986).
4. A. Brandt and A. A. Lubrecht, Multilevel matrix multiplication and fast solution of integral equations, *J. Comput. Phys.* **90**, 348 (1990).
5. J. Carrier, L. Greengard, and V. Rokhlin, A fast adaptive multipole algorithm for particle simulations, *SIAM J. Sci. Statist. Comput.* **9**, 669 (1988).
6. A. J. Degregoria and L. W. Schwartz, A boundary-integral method for two-phase displacement in Hele–Shaw cells, *J. Fluid. Mech.* **164**, 383 (1986).
7. L. M. Delves and J. L. Mohamed, *Computational Methods for Integral Equations* (Cambridge Univ. Press, Cambridge, UK, 1985).
8. G. B. Folland, *Introduction to Partial Differential Equations* (Princeton Univ. Press, Princeton, NJ, 1976).
9. P. R. Garabedian, *Partial Differential Equations* (Wiley, New York, 1964).
10. L. Greengard and V. Rokhlin, A fast algorithm for particle simulations, *J. Comput. Phys.* **73**, 325 (1987).
11. W. Hackbusch and Z. P. Nowak, On the fast matrix multiplication in the boundary element method by panel clustering, *Numer. Math.* **54**, 463 (1989).
12. M. A. Jaswon and G. T. Symm, *Integral Equation Methods in Potential Theory and Elastostatics* (Academic Press, New York, 1977).
13. O. D. Kellogg, *Foundations of Potential Theory* (Dover, New York, 1953).
14. D. Kessler, J. Koplik, and H. Levine, Numerical simulation of two-dimensional snowflake growth, *Phys. Rev. A* **30**, 2820 (1984).
15. A. Mayo, Fast high order accurate solution of Laplace's equation on irregular regions, *SIAM J. Sci. Stat. Comput.* **6**, 144 (1985).
16. A. Mayo, The fast solution of Poisson's and the biharmonic equations on general regions, *SIAM J. Numer. Anal.* **21**, 285 (1984).
17. G. B. McFadden, P. W. Voorhees, R. F. Boisvert, and D. I. Meiron, A boundary integral method for the simulation of two-dimensional particle coarsening, *J. Sci. Comput.* **1**, 117 (1986).
18. R. Menikoff and C. Zemach, Methods for numerical conformal mapping, *J. Comput. Phys.* **36**, 366 (1980).
19. S. G. Mikhlin, *Integral Equations* (Pergammon, London, 1957).
20. W. W. Mullins and R. F. Sekerka, Morphological stability of a particle growing by diffusion or heat flow, *J. Appl. Phys.* **234**, 323 (1963).
21. A. M. Odlyzko and A. Schönhage, Fast algorithms for multiple evaluations of the Riemann zeta function, *Trans. Am. Math. Soc.* **309**, 797 (1988).
22. V. Rokhlin, Rapid solution of integral equations of classical potential theory, *J. Comput. Phys.* **60**, 187 (1985).
23. Y. Saad and M. H. Schultz, GMRES: A generalized minimum residual

algorithm for solving nonsymmetric linear systems, *SIAM J. Sci. Stat. Comput.* **7**, 856 (1986).

24. M. J. Shelley, A case of singularity formation in vortex sheet motion studied by a spectrally accurate method, *J. Fluid Mech.* **244**, 493 (1992).
25. A. Sidi and M. Israeli, Quadrature methods for periodic singular and weakly singular Fredholm integral equations, *J. Sci. Comput.* **3**, 201 (1988).
26. L. van Dommelen and E. A. Rundensteiner, Fast, adaptive summation of point forces in the two-dimensional Poisson equation, *J. Comput. Phys.* **83**, 126 (1989).
27. P. W. Voorhees, G. B. McFadden, R. F. Boisvert, and D. I. Meiron, Numerical simulation of morphological development during Ostwald ripening, *Acta Metall.* **36**, 207 (1988).
28. N. J. Zabusky, M. H. Hughes, and K. V. Roberts, Contour dynamics for the Euler equations in two dimensions, *J. Comput. Phys.* **30**, 96 (1979).